Pressure, Temperature, and Thickness Dependence of CO_2-Induced Devitrification of Polymer Films

Joseph Q. Pham,[1] Stephen M. Sirard,[2] Keith P. Johnston,[1] and Peter F. Green[1,2]

[1]*Graduate Program in Materials Science and Engineering, University of Texas at Austin, Austin, Texas 78712, USA*

[2]*Department of Chemical Engineering and Texas Materials Institute, University of Texas at Austin, Austin, Texas 78712, USA*

(Received 9 December 2002; published 23 October 2003)

The glass transition temperature is known to increase with decreasing film thickness h for sufficiently thin poly(methyl methacrylate) films supported by silicon oxide substrates. We show that this system undergoes a CO_2 pressure-induced devitrification transition, P_g, which is film thickness dependent, $P_g(h) = \Delta P_g + P_g^{\text{bulk}}$. P_g^{bulk} is the bulk glass transition and ΔP_g can be positive or negative depending on T and P. The phenomenon of retrograde vitrification, wherein the polymer exhibits a rubbery-to-glassy-to-rubbery transition upon changing temperature isobarically, is also shown to occur in this system and it is film thickness dependent.

DOI: 10.1103/PhysRevLett.91.175503 PACS numbers: 61.41.+e, 61.20.Lc

Thin films play an important role in various chemical, biological, and microelectronic processes, with applications ranging from coatings to organic electronic and sensor technologies. Entropic effects (confinement), enthalpic, polymer-"wall" (substrate and free surface) interactions, and various interfacial processes associated with long-range van der Walls interactions are responsible for a range of phenomena in thin films, not observed in the bulk [1–15]. Prominent among these effects is a film thickness dependence of the vitrification temperature, shown to exist in sufficiently thin polymer films [1,2,4–6].

The effects of near-critical CO_2 on the glass transition of thin polymer films are of interest in this paper. CO_2 has also been shown to influence the phase behavior of polymer-polymer mixtures [16]. Liquid and supercritical carbon dioxide (CO_2) are attractive, nontoxic, alternatives to organic solvents in many polymer processes such as foaming, impregnation, "green" lithographic processes, and synthesis [17–19]. Moreover, because of its negligible surface tension, supercritical CO_2 is effective at drying aqueous-based photoresist films without collapsing the high-aspect ratio features with dimensions below 150 nm, a problem associated with the use of organic solvents [18]. With this in mind, it is noteworthy that the effect of CO_2 on the glass transition of thin polymer films, a central issue associated with these processes, has received little attention [10].

In thin polymer films, the vitrification transition is known to differ from the bulk transition T_g^{bulk}, $\Delta T_g = T_g(h) - T_g^{\text{bulk}}$, where ΔT_g may be positive or negative, depending on the polymer and the substrate. For freely standing films, on the other hand, $\Delta T_g < 0$ [4]. Generally, $\Delta T_g > 0$ when monomer-substrate interactions are comparatively strong, such as hydrogen bonding between monomer segmental groups and the substrate. Interactions between polyvinyl pyridine, poly(methyl methacrylate) (PMMA), tetramethyl bisphenol polycarbonate, and oxidized silicon wafers (SiO_x/Si) are examples [2,5,13]. In the absence of specific monomer-substrate interactions, as is the case for polystyrene/SiO_x/Si, $\Delta T_g < 0$ [2,5,6]. These examples illustrate that ΔT_g is not an intrinsic property of the polymer.

The origins of the film thickness dependence of T_g are still a matter of debate. Simulations suggest that the monomer packing densities determine the sign of ΔT_g [1]. Other explanations such as the existence of multiple glass transition temperatures [6] or "liquidlike" surface layers [2] provide the basis for alternate explanations. The influence of dynamic heterogeneity on vitrification of the system has also been considered as a potential explanation [20]. Most of the experimental work on this topic has concentrated on pure homopolymer systems and, more importantly, temperature is the only variable used to control vitrification. In light of the limited experimental information, it is not surprising that predictions based on each of the proposals mentioned heretofore are consistent with much of the experimental data. Experiments that reveal more systematic information about the vitrification transition, including conditions under which it could be induced, would be helpful toward the development of a better understanding of the phenomenon. Recently, we showed evidence of a CO_2-induced devitrification transition in PMMA thin films ($h > 85$ nm), suggesting that pressure provides an additional "lever" which can be used to systematically control the vitrification transition in polymer thin films [10].

In this paper we show evidence of a film thickness dependence of the CO_2 pressure-induced devitrification transition of ultrathin PMMA films supported by SiO_x/Si substrates, $P_g(h) = \Delta P_g + P_g^{\text{bulk}}$, where P_g^{bulk} is the bulk transition. The magnitude and sign of ΔP_g can be controlled independently by T and P. This observation has implications regarding the additional role of diluent interactions on the devitrification of thin films. Moreover, a retrograde vitrification envelope is shown to exist in

this system. The polymer undergoes a transition from rubbery-to-glassy-to-rubbery upon changing temperature isobarically. The maximum pressure associated with the envelope shifts to lower pressures when h becomes sufficiently small.

PMMA ($M_w = 227$ kg/mol; $M_w/M_n = 1.04$), purchased from Polysciences Inc., was dissolved in toluene and spin cast onto cleaned silicon (100) wafers (Wafer World Inc.). The silicon substrate had a native SiO_x layer thickness of $\sim$1.5 nm, as determined by spectroscopic ellipsometry. The films ranged in thickness between 10 and 200 nm. All samples were annealed at 170 °C under vacuum for over 24 h to remove residual solvent and to establish the same thermal history.

Measurements were performed using a variable angle spectroscopic ellipsometer (J. A. Woollam Co.). High-pressure ellipsometry cells were used to measure the CO_2-induced glass transitions of PMMA at different film thicknesses at two temperatures: 35 and 75 °C. In addition, P_g's were measured for samples of thicknesses $h = 15$ nm and $h = 80$ nm at additional temperatures of 25, 50, and 100 °C. The design of the cells and the experimental setup may be found elsewhere [9,10]. For thick films ($h > 30$ nm), the measurements were made using an angle of incidence of 70° from the vertical, while an angle of 76° was used for thinner films. Once a sample was loaded in the cell, at least 1 h was allowed for thermal equilibration. The temperature was controlled with an accuracy of ± 0.2 °C. After reaching thermal equilibrium, ellipsometric angles, ψ and Δ, were measured for different CO_2 (Air Products; $> 99.9999\%$ purity) pressures for both sorption and desorption. The pressure was controlled with an accuracy of ± 0.2 bars. Each sample was equilibrated at each pressure for 10–20 min.

Studies of the solubility/dilation of CO_2 in bulk conditioned polymers indicate that at pressures, P, below the $P_g(h)$, sorption and desorption isotherms exhibit negative curvature as a function of P. Furthermore, a hysteresis is observed for $P < P_g$ between the initial sorption isotherms for the unconditioned glassy polymer and the subsequent desorption/sorption isotherms on the conditioned polymer. In contrast, for $P > P_g$, the isotherms are reversible and exhibit positive curvature [12,21,22]. The pressure at which the change in curvature occurs is identified as the P_g (i.e., sufficient CO_2 is absorbed by the polymer to induce a devitrification transition). In conditioned samples, subsequent sorption and desorption runs give the same transition.

We measured the ellipsometric angle ψ as a function of CO_2 pressure at different wavelengths (from 400 to 700 nm) for both sorption and desorption isotherms. Since ψ is related to the film thickness, it also exhibits a change in curvature, denoting the onset of P_g. We find that the P_g's determined for the thickest films compare favorably to the related bulk values, demonstrating that the P_g for the thin films can be determined by spectroscopic ellipsometry without explicitly fitting the ellipsometric angles to a model. Furthermore, a hysteresis is also observed between the initial sorption isotherms and the subsequent sorption and desorption isotherms at $P < P_g$, supporting the observation that a glass transition is present. All data presented in this paper were determined by using ψ's from initial desorption isotherms. Typical ψ versus CO_2 pressure desorption isotherms for film thickness of $h = 26$ nm and $h = 50$ nm are shown in Figs. 1(a) and 1(b). The trends in the data in each figure clearly reveal distinct glassy and rubbery regimes. Before concluding the experimental section is it important to note that an anomalous dilation is exhibited by the films at pressures higher than the P_g's [10]. This anomalous dilation behavior is associated with the compressibility of the

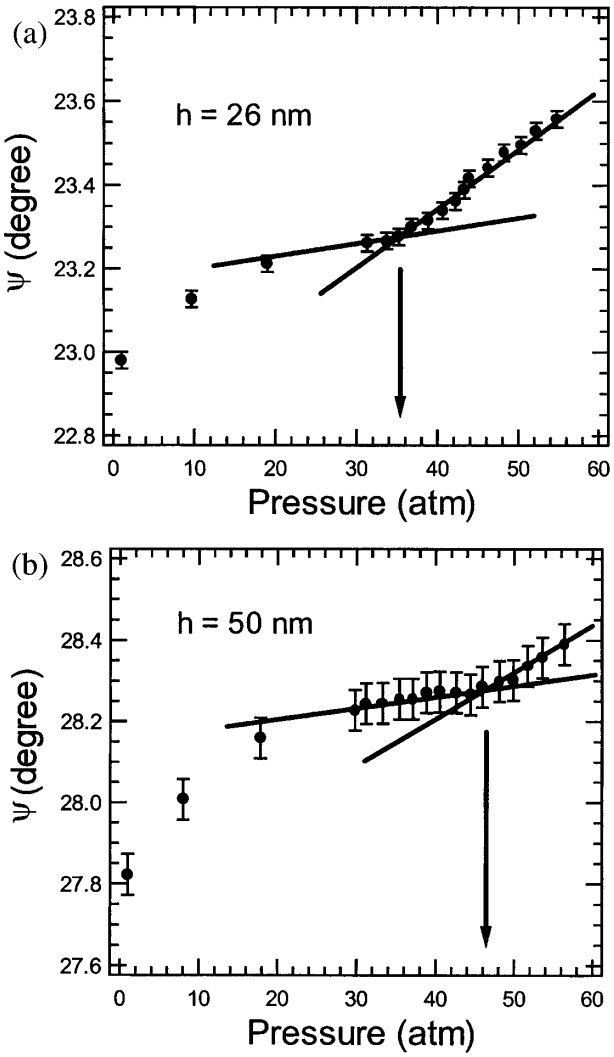

FIG. 1. Typical ellipsometric angle (ψ) versus CO_2 pressure plots are shown here for two different PMMA film thicknesses, (a) 26 nm and (b) 50 nm at 75 °C. The CO_2-induced glass transition, P_g, is identified as the pressure at which the curvature of the desorption isotherm changes.

solvent, whereas the measured P_g is evidently not correlated with the solvent compressibility [15].

Three important observations are apparent from the data in Fig. 2. (1) The P_g's at 35 and 75 °C decrease with decreasing film thickness, $\Delta P_g < 0$, for h less than ~50 nm, indicating that lower pressures are required to induce devitrification in thinner films. These P_g's are independent of film thickness at large h. (2) A larger pressure is required to induce the devitrification transition at 35 °C than at the higher temperature of 75 °C. (3) The change in ΔP_g with decreasing h is larger at 75 °C than at 35 °C [$\Delta P_g(75\,^\circ\mathrm{C}) > \Delta P_g(35\,^\circ\mathrm{C})$].

We begin by discussing the film thickness dependence of P_g. The decrease of the devitrification transition with decreasing h is, at first glance, surprising based on the dependence of the transition on film thickness for the pure (solventless) PMMA/SiO_x/Si case. In the solventless case, the interactions (hydrogen bonding) of the atactic PMMA with the SiO_x layer are implicated for the increase in the transition over the bulk. The effect of the enhanced interactions is to increase the local monomer-monomer density in the vicinity of the substrate [1,5,7,8,14]. An associated effect is that the mobility of chain segments in the vicinity of the substrate is reduced. Therefore one might assume that the devitrification transition would occur at higher pressures with decreasing h. In the case of CO_2-PMMA/SiO_x/Si, CO_2 interacts with the carbonyl groups of PMMA, plasticizing the system [19,23]. This alone would have the effect of changing the effective PMMA/SiO_x interactions, and hence, the configuration freedom on the chains in the vicinity of the substrate. In fact, CO_2 also interacts with the hydroxyl groups on the substrate [19,23–25]. Therefore it is reasonable to argue that the interactions of PMMA with the surface silanol groups will be screened in the presence of CO_2. One natural consequence of this would be the mediation of the influence of the "interacting" substrate on the segmental packing density and hence the mobility of chain segments. A third effect is the high concentration of CO_2 at the surface (adsorption) of the film [9–11,26]. This has the effect of providing more configurational freedom to chain segments near the free surface. These effects, collectively, induce the devitrification transition to occur at lower pressures with decreasing film thickness. While interactions between the chain segments and the external interfaces are fundamentally associated with the thickness dependent vitrification transitions, it should also be evident that the collective dynamics and segmental distributions throughout the entire film would be affected.

The reason that the $P_g(h)$ versus h isotherms shift to higher pressures as the temperature decreases from 75 to 35 °C is associated with the fact that a greater solubility of CO_2 in the PMMA is required to counterbalance the decrease in thermal motion. The data at large h are consistent with independent measurements performed on bulk samples [27]. The difference in the film thickness effects on the glass transition at the two temperatures $\Delta P_g(75\,^\circ\mathrm{C}) > \Delta P_g(35\,^\circ\mathrm{C})$ is due in part to the distribution of CO_2 between the surfaces and the interior of the film. At 35 °C the solubilities of CO_2 are much higher than at 75 °C over the pressure ranges studied. Thus the gradient in CO_2 composition from the interior of the film to the free surface may be expected to be smaller at 35 °C than at 75 °C (i.e., the difference between the average concentrations of CO_2 in thick and thin films is smaller at 35 °C than at 75 °C) consistent with a smaller ΔP_g at 35 °C.

A retrograde vitrification phenomenon as shown in Fig. 3, wherein at constant pressure the system exhibits rubbery-glassy transitions at two different temperatures, is observed in this system. The vitrification envelope is shown here for the bulk and for thin $h = 80$ nm and $h = 15$ nm films. The behavior of the $h = 80$ nm films is nearly the same as the bulk, consistent with the thickness dependence of the P_g shown in Fig. 2. It is noteworthy that the envelope shifts to lower pressures, by

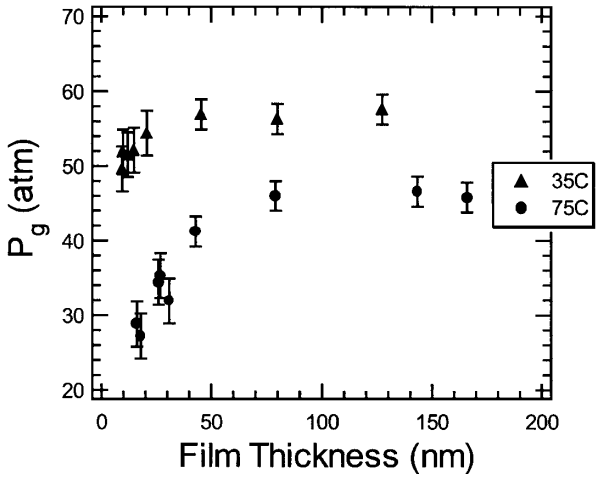

FIG. 2. P_g is shown here as a function of h at 35 and 75 °C.

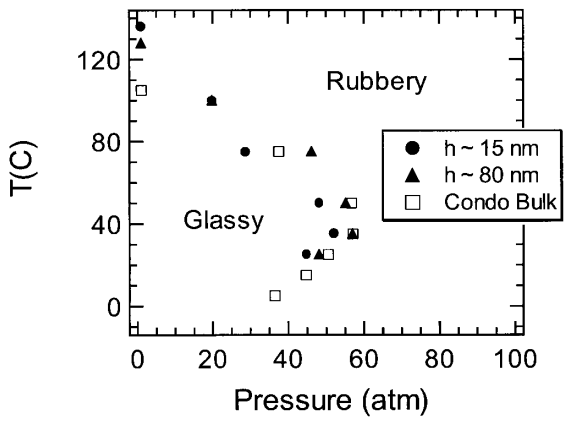

FIG. 3. Temperature versus pressure plots are shown here for bulk PMMA (from Ref. [27]) and for films of $h \sim 15$ nm and $h \sim 80$ nm.

~10–20 bars, for the thinnest film. Retrograde vitrification is associated with the increasing CO_2 solubility in the polymer with decreasing temperature. At high temperatures and low pressures, the rubbery state is associated with the availability of sufficient thermal energy and mobility of chain segments. As the temperature is reduced isobarically, vitrification occurs for the typical reasons associated with the time scale of the dynamics versus the time scale of observation (loss of ergodicity). However, as the temperature is reduced further, the solubility of CO_2 increases appreciably, resulting in the plasticization of the film at lower T, i.e., devitrification. In this regard, the explanation of the phenomenon in thin films is the same as that for the bulk. However, the envelope shifts to lower pressures for thin films. This shift is associated with reasons provided earlier, the decreasing devitrification transition with decreasing h.

We note the existence of a crossover at high T and low P, which is not unexpected. At ~20 atm and $T \sim 100\,^{\circ}\mathrm{C}$, a crossover occurs, where the vitrification transition occurs at the same temperature and pressure for thin films and bulk. At pressures lower than ~20 atm, vitrification increases with decreasing film thickness. This occurs in the regime where the CO_2 solubility is very low. Indeed, one should eventually arrive at a crossover transition where the behavior of the solventless case is recovered.

We have shown that the vitrification transition in PMMA thin films could be controlled by changing the conditions of temperature and CO_2 pressure. A novel crossover pressure is presented in which the sign of ΔP_g changes due to the interactions among polymer, solvent, and substrate at the interfaces. Furthermore, the phenomenon of retrograde vitrification occurs in the CO_2/PMMA/SiO_x/Si system, wherein upon decreasing temperature, isobarically, PMMA undergoes a rubbery-to-glassy transition and upon a further decrease, a glassy-to-rubbery transition occurs. This phenomenon is associated with the interplay between the increasing thermal energy of the system with increasing temperature and the increasing CO_2 solubility in the system with decreasing temperature. The vitrification envelope shifts to lower pressures by 10–20 atm when the films are sufficiently thin. The results presented here not only have important implications regarding CO_2-based semiconductor processing and gas separation membranes in polymer based systems, but they provide an important basis for the further development of theories of the glass transition in thin polymeric films.

This work was supported by the National Science Foundation (DMR-0072898) and by the STC Program of the National Science Foundation under Agreement No. CHE-9876674.

[1] J. D. McCoy and J. G. Curro, J. Chem. Phys. **116**, 9154 (2002).
[2] J. L. Keddie, R. A. Jones, and R. A. Cory, Europhys. Lett. **27**, 59 (1994).
[3] K. Binder, Adv. Polym. Sci. **112**, 181 (1994).
[4] J. A. Forrest and K. Dalnoki-Veress, Adv. Colloid Interface Sci. **94**, 167 (2001).
[5] J. A. Torres, P. F. Nealy, and J. J. de Pablo, Phys. Rev. Lett. **85**, 3221 (2000).
[6] J. H. Kim, J. Jang, and W-C. Zin, Langmuir **17**, 2703 (2001); **16**, 4064 (2000).
[7] K. F. Mansfield and D. N. Theodorou, Macromolecules **24**, 6283 (1991).
[8] J. Baschnagel and K. Binder, Macromolecules **28**, 6808 (1995); I. Bitsanis and G. Hadziioannous, J. Chem. Phys. **92**, 3827 (1990).
[9] S. M. Sirard, P. F. Green, and K. P. Johnston, J. Phys. Chem. B **105**, 766 (2001).
[10] S. M. Sirard, K. J. Zeigler, I. C. Sanchez, P. F. Green, and K. P. Johnston, Macromolecules **35**, 1928 (2002).
[11] S. M. Sirard, R. R. Gupta, T. P. Russell, J. J. Watkins, P. F. Green, and K. P. Johnston, Macromolecules **36**, 3365 (2003).
[12] Y. Kamiya, K. Mizoguchi, and Y. Naito, J. Polym. Sci., Part B, Polym. Phys. **24**, 535 (1986).
[13] J. Q. Pham and P. F. Green, Macromolecules **36**, 1665 (2003).
[14] A. van der Lee, Langmuir **17**, 7664 (2001).
[15] W. Wu, C. F. Majkrzak, S. K. Satija, J. F. Ankner, W. J. Orts, M. Satkowski, and S. D. Smith, Polymer **33**, 5081 (1992).
[16] J. J. Watkins, G. D. Brown, V. S. Ramachandra Rao, M. A. Pollard, and T. P. Russell, Macromolecules **32**, 7737 (1999).
[17] S. L. Wells and J. DeSimone, Angew. Chem. **40**, 518 (2001).
[18] G. L. Weibel and C. K. Ober, Microelectron. Eng. **65**, 145 (2003); H. Namatsu, J. Vac. Sci. Technol. B **18**, 3308 (2000).
[19] S. G. Kazarian, M. F. Vincent, F.V. Bright, C. L. Liotta, and C. A. Eckert, J. Am. Chem. Soc. **118**, 1729 (1996).
[20] D. Long and F. Lequeux, Eur. Phys. J. E **4**, 371 (2001).
[21] W. J. Koros and D. R. Paul, J. Polym. Sci., Polym. Phys. Ed. **16**, 1947 (1978).
[22] R. G. Wissinger and M. E. Paulaitis, J. Polym. Sci., Part B: Polym. Phys. **25**, 2497 (1987).
[23] C. P. Tripp and J. R. Combes, Langmuir **14**, 7384 (1998).
[24] J. R. Strubinger and J. F. Pratcher, Anal. Chem. **61**, 951 (1989); J. R. Strubinger, H. Song, and J. F. Pratcher, Anal. Chem. **63**, 98 (1991).
[25] X. Jia and T. J. McCarthy, Langmuir **18**, 683 (2002).
[26] G. H. Findenegg, *Fundamentals of Adsorption*, edited by A. L. Meyers and G. Belfort (Engineering Foundation, New York, 1984), p. 207.
[27] P. D. Condo, D. R. Paul, and K. P. Johnston, Macromolecules **27**, 365 (1994); P. D. Condo and K. P. Johnston, Macromolecules **25**, 6730 (1992).